In einer anderen Arbeit [9] wurde 9,20 eV gefunden.

Besondere Sorgfalt wurde weiter auf die Bestimmung der IP von C_6H_4 und C_6H_2 verwandt, die besonderes Interesse beanspruchen können. Für C_6H_4 ergab sich als Mittelwert aus 18 Messungen aus 8 verschiedenen aromatischen Molekülen:

$$9{,}50 \pm 0{,}15 \text{ eV}$$

und für C_6H_2 als Mittelwert aus 6 Messungen an 3 verschiedenen Molekülen:

$$9{,}85 \pm 0{,}15 \text{ eV}.$$

Abb. 1 zeigt die Meßkurven für die IP von C_6H_5 und C_6H_4, die durch Elektronenstoß aus Antimontriphenyl gebildet wurden.

Herrn Prof. W. Paul, der diese Arbeit zu jeder Zeit unterstützt und gefördert hat, danken wir für anregende Diskussionen.

Dem Landesamt für Forschung des Landes Nordrhein-Westfalen schulden wir Dank für finanzielle Unterstützung.

Mass Spectrometry: The Shapes of "Meta-Stable Peaks"

J. H. Beynon and A. E. Fontaine

Imperial Chemical Industries Limited, Dyestuffs Division, Blackley, Manchester, England

(Z. Naturforschg. **22 a**, 334—346 [1967]; received 26 November 1966)

The effect on the shape of "metastable peaks" arising from decompositions throughout the whole flight path in a mass spectrometer is considered. The effects of discriminations against product ions are calculated; the effects of finite beam dimensions, angular spreading and kinetic energy of separation of fragments during the decomposition are discussed theoretically and illustrated by practical examples.

"Meta-stable peaks" are defined as peaks arising in mass spectra due to decomposition of meta-stable ions during their flight through the mass spectrometer tube. They are recognisable in mass spectra not only from the fact that they appear at non-integral mass numbers, but also because they are more diffuse than the normal mass peaks due to ions which travel the whole length of the spectrometer without decomposition. The shapes of "meta-stable peaks" are sometimes difficult to observe because of the overlap which occurs with normal peaks in the same region of the mass spectrum. Fig. 1 shows part of the mass spectrum of 2-ethyl piperidine including the region below mass 12. In this region of the spectrum there is little interference from normal mass peaks and the shapes of the "meta-stable peaks" can be more easily observed. It can be seen that the peaks are of varying widths and shapes. Although the shape of most "meta-stable peaks" observed in the mass spectra of organic compounds is roughly Gaussian, even these peaks differ widely in width. In addition, peaks having "flat tops" [1] or "dished tops" [2] as well as more complex asymmetric shapes are often observed, sometimes in the same mass spectrum.

There have been several previous papers dealing with "meta-stable peaks". Barber and Elliott [3] have discussed the relative sensitivities of single and double focussing geometries in the detection of daughter ions from meta-stable decompositions occurring in the region immediately preceding the magnetic analyser. The exact position at which "meta-stable peaks" appear on the mass scale has been discussed by Momigny [4] and Flowers [5]. In these laboratories we have considered [1] the effect on peak shape of decompositions which involve kinetic energy of separation of the fragments, but the treatment was a simplified one in which energy release only along the direction of motion of the ions was considered. The width of a "flat topped meta-stable peak" can be correlated with the energy released but there was no discussion of the detailed shape of the

[1] J. H. Beynon, R. A. Saunders, and A. E. Williams, Z. Naturforschg. **20 a**, 180 [1965].
[2] W. Higgins and K. R. Jennings, Trans. Faraday Soc. **62**, 97 [1966].
[3] M. Barber and R. M. Elliott, 12th Annual Conference on Mass Spectrometry and Allied Topics. Committee E. 14 A.S.T.M. Montreal, June 1964.
[4] J. Momigny, Private Communication 1964.
[5] M. C. Flowers, Chem. Comm. 235 [1965].

peak produced. JENNINGS and HIGGINS [2] have reported decompositions of doubly charged ions. In such decompositions, due to the energy of separation of the two positive charges [6], a large energy release of the order of a few electron volts is observed. This causes the "meta-stable peak" to develop a "dished" top and MCLAFFERTY et al. [7] have shown that in certain decompositions giving lower energy release the shape of the top of a "meta-stable peak" can change from "flat" to "dished" shape as the energy of the meta-stable ion is decreased.

Recent calculations by ELLIOTT [8] and FLOWERS [5] have taken into account the possibility of the energy release in a meta-stable decomposition producing a velocity component in the daughter ion directed at an angle to the direction of flight of the precursor ion. Both these workers have developed equations related to the geometry of the A.E.I. Limited type M.S. 9 [9] mass spectrometer which claimed to give information on the width and profile of a "meta-stable peak" in terms of this angle, the distance travelled in the field free region before decomposition, and the amount of energy released. Both equations predict a steeply "dished top" peak.

Decompositions occurring within the electrostatic analyser of a double-focussing mass spectrometer of NIER–JOHNSON geometry have also been reported by BARBER and ELLIOTT [3] and by BEYNON, SAUNDERS and WILLIAMS [10]. It was shown that the result of such decompositions is to produce a broadened "meta-stable peak" which extends upwards in mass from a mass m_2^2/m_1 towards m_2 where m_1 is the mass of the meta-stable ion and m_2 the mass of the daughter ion formed in the decomposition. The extent of the spread in mass depends on the energy discrimination of this stage of the mass spectrometer.

It is a simple matter to introduce wiring modifications to allow a large, precise and continuous variation in the ratio of accelerating to deflecting voltage and to allow only daughter ions which have been formed in the field free region preceding the electrostatic analyser to be recorded. The "meta-stable peaks" then observed are better focussed and more intense than those produced in conventional spectra and this technique of studying meta-stable ion decompositions has been used successfully by JENNINGS [11] with NIER–JOHNSON geometry and by FUTTRELL and co-workers with MATTAUCH–HERZOG ion optics [12]. JENNINGS [13] has further used this modification to observe a product ion which has been formed as a result of two decompositions along a flight path. An arrangement closely resembling that of JENNINGS and of FUTRELL has been used by OSBERGHAUS and OTTINGER to measure fragmentation energies in hydrocarbons [14, 15].

BECKEY has reported meta-stable decompositions observed in field ionisation mass spectra [16] using a single-focussing mass spectrometer and he cites [17] many examples of intense "meta-stable peaks" due to decompositions in the field free region. "Meta-stable peaks" in field ionisation mass spectra have also been reported in these laboratories [18] and by ROBERTSON [19].

It is the purpose of this paper to consider in more detail the conditions which give rise to "meta-stable peaks" of different shapes and also to investigate regions of the flight path which have not been considered by previous workers. The analysis has been mainly restricted to considerations of a single-focussing sector type geometry and detailed attention has not been paid to the field free regions preceding the electrostatic analyser in double-focussing instruments, although decompositions here are discussed qualitatively. A mass spectrometer may be considered as divided into the following regions:

(a) The accelerating region.

(b) The field free region preceding the electrostatic analyser and the electrostatic analyser (for double-focussing instruments).

[6] J. H. BEYNON and A. E. FONTAINE, Chem. Comm. 717 [1966].
[7] T. W. SHANNON, F. W. MCLAFFERTY, and C. R. MCKINNEY, Chem. Comm. 478 [1966].
[8] R. M. ELLIOTT, Private Communication 1965.
[9] R. D. CRAIG, B. N. GREEN, and J. D. WALDRON, Chimia **17**, 33 [1963].
[10] J. H. BEYNON, R. A. SAUNDERS, and A. E. WILLIAMS, Nature **204**, 67 [1964].
[11] K. R. JENNINGS, J. Chem. Phys. **43**, 4176 [1965].
[12] J. H. FUTTRELL, K. R. RYAN, and L. W. SIECK, J. Chem. Phys. **43**, 1832 [1965].
[13] K. R. JENNINGS, Chem. Comm. 283 [1966].
[14] CH. OTTINGER and O. OSBERGHAUS, Physics Letters **17**, 269 [1965].
[15] CH. OTTINGER, Z. Naturforschg. **20 a**, 1229 [1965].
[16] H. D. BECKEY, Bull. Soc. Chim. Belges **73**, 326 [1964].
[17] H. D. BECKEY, in "Mass Spectrometry" A N.A.T.O. Advanced study institute on theory, design and appplications, Glasgow 1964. Ed. R. I. REED, Academic Press 1965.
[18] J. H. BEYNON, A. E. FONTAINE, and B. E. JOB, Z. Naturforschg. **21 a**, 776 [1966].
[19] A. J. ROBERTSON and B. W. VINEY, Advances in Mass Spectrometry, Vol. III, published by The Institute of Petroleum, London 1966.

(c) The field free region in front of the magnetic analyser.

(d) The region within the dispersing (sector) magnetic field.

(e) The field free region between the magnetic field and the collector slit.

Theoretical

a) Decompositions of meta-stable ions in the accelerating field

HIPPLE and CONDON [20] showed that in a magnetic sector mass spectrometer the ion m_2^+ from the decomposition of a meta-stable ion m_1^+ appears on the mass scale at m^* where

$$m^* = \frac{m_2^2}{m_1}\left[1 + \frac{(m_1 - m_2)(V - V^1)}{m_2 V}\right].$$

V is the full accelerating voltage available and V^1 is the potential through which the ion m_1^+ has fallen before decomposition occurs. The equation shows that as V^1 increases from zero to V, m^* varies in value from m_2 to m_2^2/m_1. The equation assumes that there is no kinetic energy of separation of the fragments at decomposition. In order to calculate the peak shape at m^* it is necessary to know the shape of the accelerating field, since this will affect the efficiency of transmission of the product ions m_2^+ through the entrance slit of the mass spectrometer and also to apply a weighting factor to each individual decomposition dependent on the velocity of m_1 at the moment of decomposition. This velocity and the field shape at V^1 will determine the interval of time spent by m_1^+ in this region. For the very simple case of a uniform field, m^* will take the form of a continuum extending the entire distance from m_2 to m_2^2/m_1 the intensity increasing towards m_2 because of the weighting factor discussed above.

If m_1^+ decomposes at a very small value of V^1 the daughter ion will arrive at the entrance slit of the mass spectrometer with almost the full accelerating energy. Discriminations against such ions will therefore be small and they will appear as a tail on the low mass side of m_2.

If m_1^+ decomposes when $V^1 \cong V$ the ion is near enough to the slit to be likely to pass through it, even though in the decomposition it loses a fraction $(m_1 - m_2)/m_1$ of its energy. Such ions will appear in the tail on the high mass side of m^*. Ions reaching the entrance slit with intermediate energies would be expected to suffer more discrimination in a non-uniform field.

There will be interference to observation of these effects due to the fact that there is a continuum which extends from mass m_2^2/m_1 through m_2 to m_1. This is due to decompositions which occur within the magnetic field and is discussed in Section d.

If there is a release of T eV of kinetic energy at the moment of decomposition, so that the fragmentation can be represented by:

$$m_1^+ \rightarrow m_2^+ + (m_1 - m_2) + T \text{ eV}$$

discriminations in passing through the entrance slit will be increased, but ions which pass through the slit will again give rise to a continuum from m^* to m_2.

b) Decomposition of meta-stable ions in the field free region before the electrostatic analyser and the region within the electrostatic analyser (Double-focussing instrument)

In general, daughter ions from decompositions occurring in this region of a double-focussing mass spectrometer will not reach the collector since they have not the correct energy to pass through the electrostatic analyser. The energy pass band of this analyser is, however, finite and the daughter ions from decompositions involving very small mass changes (1.3% for the M.S. 9) occurring before the electrostatic analyser can pass through and appear in the normal mass spectrum. The situation obtaining for decomposition within the electrostatic analyser has been described elsewhere [10], and no further discussion of decomposition in this region will be given here.

c) Decomposition of meta-stable ions in the field free region in front of the magnetic analyser

Fig. 2 is a schematic diagram of the magnetic sector of a single focussing 90° mass spectrometer. The magnetic field is uniform over the area of the magnet and in a direction perpendicular to the plane of the paper (this direction is identified as the z direction). The x direction is defined as the direction of motion of ions which enter the magnet perpendicular to the pole face and which describe an arc of radius R, leaving the magnet also perpendicu-

[20] J. A. HIPPLE and E. U. CONDON, Phys. Rev. **69**, 347 [1946].

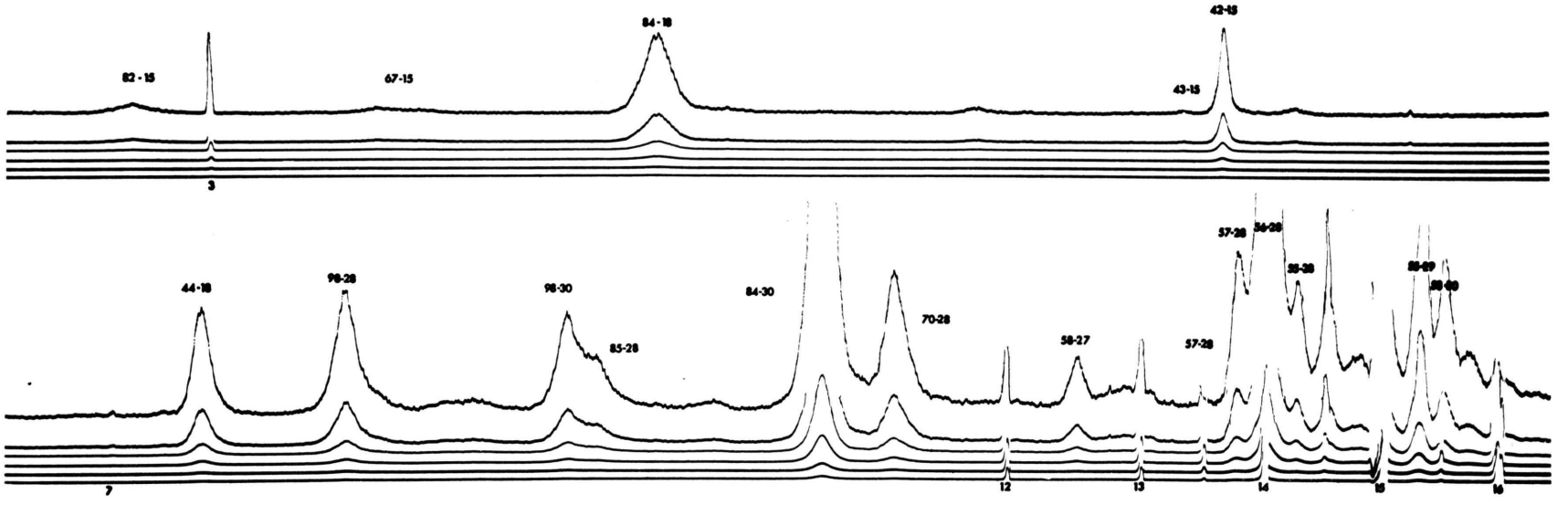

Fig. 1. The mass spectrum of 2-ethyl piperidine below mass 16 showing several different widths of a "meta-stable peaks"; e. g. 82-15 denotes a peak due to the decomposition $82^+ \rightarrow 15^+ + 67$.

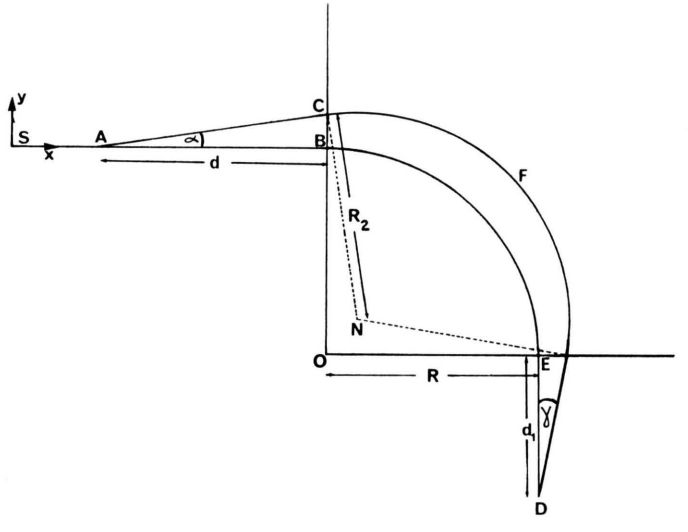

Fig. 2. Schematic diagram showing decompositions occurring in the field free space in front of the magnetic analyser with release of kinetic energy.

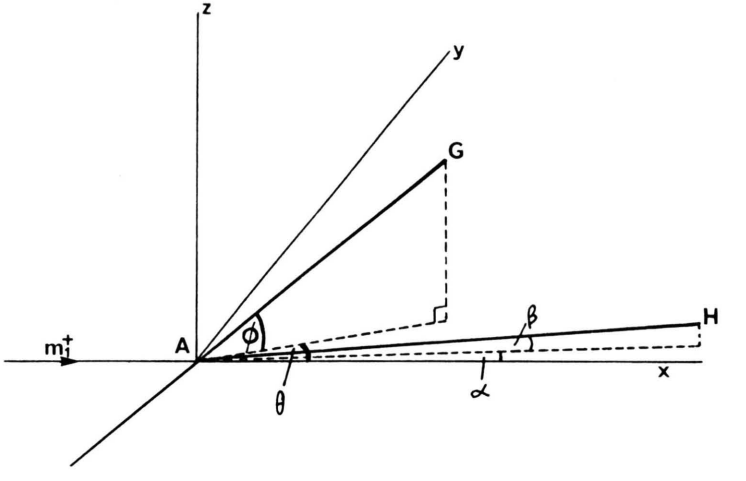

Fig. 3. The co-ordinate system used to define the direction of motion of the daughter ion m_2^+ in terms of the direction of momentum changes on decomposition.

lar to a pole face before entering the collector slit. The y direction is perpendicular to both the x and z directions. The lengths of the slits of the mass spectrometer lie in the z direction.

Let A represent the site of decomposition of a meta-stable ion according to

$$m_1^+ \rightarrow m_2^+ + (m_1 - m_2) + T$$

where T represents the release of kinetic energy in the fragmentation. Let m_1^+ have a kinetic energy E_0 immediately before decomposition and be moving in the x-direction. The ion m_2^+ will in general have a velocity in the xy plane of magnitude V_α which makes an angle α with the x-direction. Considering only the component of velocity in this plane, m_1^+ follows the path AC to the magnet.

Let $\frac{1}{2} m_2 V_\alpha^2 = E_\alpha$.

Let m_2^+ move in the magnetic field in the arc CF of radius R_2 which brings it to the collector along a path making an angle γ with the normal to the magnet pole face, and let the magnetic field at which this occurs be H_α. R_2 can be evaluated from the geometrical relationships:

$$(R + d \operatorname{tg} \alpha)^2 + (R + d_1 \operatorname{tg} \gamma)^2 = 2 R_2^2 (1 + \sin(\gamma + \alpha)), \qquad (1)$$

$$R_2 = \frac{R + d \operatorname{tg} \alpha}{\cos \alpha + \sin \gamma}. \qquad (2)$$

Simultaneously with the collection of m_2^+ let an ion of mass m^* with energy E_0 move along the path SABED and also reach the collector without suffering decomposition en-route. Thus for m^*

$$R^2 = \frac{2 E_0 m^*}{H_\alpha^2 e^2},$$

where e is the electronic charge, and for m_2^+

$$R_2^2 = \frac{2 E_\alpha m_2}{H_\alpha^2 e^2}.$$

Hence

$$m^* = m_2 \frac{E_\alpha}{E_0} \frac{R^2}{R_2^2}. \qquad (3)$$

m^* is the apparent mass of the ion m_2^+.

The situation at the moment of decomposition of m_1^+ is shown in more detail in Fig. 3. The momentum changes resulting from the released energy T are directed along the vector AG. The vector AG makes an angle Θ to the x-axis in the xy plane and an angle Φ to the xy plane. Let the final direction of motion of m_2 be represented by the vector AH making corresponding angles α and β in the xy plane and perpendicular to it. Let V_1, the velocity of m_1 before decomposition be resolved into three components, V_{1a} along the vector AG, V_{1b} along a line in the xy plane perpendicular to AG and V_{1c} in a direction perpendicular to these two directions. Then

$$V_{1a} = V_1 \cos \Phi \cos \Theta,$$
$$V_{1b} = V_1 \sin \Theta,$$
$$V_{1c} = V_1 \sin \Phi \cos \Theta.$$

If V_{2a}, V_{2b}, V_{2c} and V_{3a}, V_{3b} and V_{3c} are respectively the three components of the velocities of m_2 and the neutral particle along the axes defined above, we can write three sets of energy and momentum equations.

$$\tfrac{1}{2} m_1 V_{1a}^2 + T = \tfrac{1}{2} m_2 V_{2a}^2 + \tfrac{1}{2} (m_1 - m_2) V_{3a}^2, \quad (4)$$
$$m_1 V_{1a} = m_2 V_{2a} + (m_1 - m_2) V_{3a}, \quad (5)$$
$$\tfrac{1}{2} m_1 V_{1b}^2 = \tfrac{1}{2} m_2 V_{2b}^2 + \tfrac{1}{2} (m_1 - m_2) V_{3b}^2, \quad (6)$$
$$m_1 V_{1b} = m_2 V_{2b} + (m_1 - m_2) V_{3b}, \quad (7)$$
$$\tfrac{1}{2} m_1 V_{1c}^2 = \tfrac{1}{2} m_2 V_{2c}^2 + \tfrac{1}{2} (m_1 - m_2) V_{3c}^2, \quad (8)$$
$$m_1 V_{1c} = m_2 V_{2c} + (m_1 - m_2) V_{3c}. \quad (9)$$

Writing $\frac{1}{2} m_1 V_{1a}^2$ as $E_0 \cos^2 \Phi \cos^2 \Theta$,
$\frac{1}{2} m_1 V_{1b}^2$ as $E_0 \sin^2 \Theta$,
$\frac{1}{2} m_1 V_{1c}^2$ as $E_0 \sin^2 \Phi \cos^2 \Theta$

the solutions for the six velocities are:

$$V_{2a} = \pm \sqrt{2 \mu T / m_1} + \cos \Phi \cos \Theta \sqrt{2 E_0 / m_1}$$
where $\mu = (m_1 - m_2)/m_2$,

$$V_{3a} = \pm \sqrt{2 T / \mu m_1} + \cos \Phi \cos \Theta \sqrt{2 E_0 / m_1},$$

$$V_{2b} = V_{3b} = \sin \Theta \sqrt{2 E_0 / m_1},$$

and

$$V_{2c} = V_{3c} = \sin \Phi \cos \Theta \sqrt{2 E_0 / m_1}.$$

The three velocity components of m_2 can now be compounded as two components, one in the z direction (V_z) and one in the xy plane at an angle α to the x direction (V_α).

$$V_\alpha^2 = (V_{2a} \cos \Phi + V_{2c} \sin \Phi)^2 + V_{2b}^2,$$
$$V_z = V_{2a} \sin \Phi - V_{2c} \cos \Phi,$$
$$\text{and } \cot(\Theta - \alpha) = \frac{V_{2a} \cos \Phi + V_{2c} \sin \Phi}{V_{2b}}$$

Substituting the values of V_{2a}, V_{2b} and V_{2c} we get:

$$V_\alpha^2 = \frac{2 E_0}{m_1} \left[1 + \frac{\mu T}{E_0} \cos^2 \Phi \pm 2 \cos \Theta \cos \Phi \sqrt{\mu T / E_0} \right], \qquad (10)$$

$$V_z = \pm \sin \Phi \sqrt{2 \mu T / m_1}\,, \qquad (11)$$

and

$$\cot \alpha = \operatorname{cosec} \Theta [\pm \sec \Phi \sqrt{E_0/\mu T} + \cos \Theta]. \qquad (12)$$

From equation (10):

$$E_\alpha = \tfrac{1}{2} m_2 V_\alpha^2 = \frac{m_2}{m_1} E_0 \left[1 + \frac{\mu T}{E_0} \cos^2 \Phi \pm 2 \cos \Theta \cos \Phi \sqrt{\mu T / E_0}\right]. \qquad (13)$$

As the magnet of the mass spectrometer produces mass dispersion only in the xy plane, we need only consider the motion of m_2^+ in this plane in order to calculate the value of m^*. Thus, substituting for E_α/E_0 in (3)

$$m^* = \frac{m_2^2}{m_1} \frac{R^2}{R_2^2} \cdot \left[1 + \frac{\mu T}{E_0} \cos^2 \Phi \pm 2 \cos \Theta \cos \Phi \sqrt{\mu T / E_0}\right]. \qquad (14)$$

In order to calculate R_2 from Eqs. (1) and (2) the value of α corresponding to any pair of Θ and Φ is required. This is obtained from Eq. (12).

To be recorded the daughter ion from the decomposition must pass through the collector slit. For this to occur for an ion diverging from the centre of the beam, the distance travelled in the z-direction must not exceed $l/2$ where l is the collector slit length. From Fig. 2 the path length in the x-direction after decomposition is given by:

$$\frac{d}{\cos \alpha} + \left(\frac{\pi}{2} + \alpha + \gamma\right) R_2 + \frac{d_1}{\cos \gamma}$$

or to a good approximation, $d + \frac{1}{2} \pi R + d_1$.

The angle subtended by the half slit length at the decomposition site is:

$$\mathrm{tg}^{-1} \frac{l}{2(d + \frac{1}{2} \pi R + d_1)}$$

and the approximate condition for collection is

$$\frac{V_z}{V_\alpha \cos \alpha} (d + \tfrac{1}{2} \pi R + d_1) \leqq l/2\,.$$

Similar conditions for collection employing the appropriate fraction of the slit length hold for daughter ions diverging from places in the beam other than the centre. The calculation of the profile of a "meta-stable peak" due to decompositions involving the release of a discrete amount of energy can now be undertaken.

Selecting triplets of values for Θ, Φ and d a computer was used to evaluate: –

α from equation (12),
R_2 from equations (1) and (2),
and m^* from equation (14).

The geometry used in the calculation was that of the M.S. 9 mass spectrometer[9] in which $R = 12''$, $d_1 = 8.47''$ and d varies from $21''$ to zero. E_0 was taken as 8000 eV. Θ varies between 0° and 360° and Φ from 0° to 90°.

It was assumed that the probability of decomposition of m_1^+ was the same over the whole path length. This is equivalent to assuming a half-life for decomposition very long compared to the time of flight. This assumption has been made throughout the paper; the consequences are discussed later. The value of m^* for any chosen set of data was calculated using an English Electric type K.D.F. 9 computer. The data used in each evaluation was subjected to the condition for collection given above. After sorting the values of m^*, the intensity distribution in the "meta-stable peak" was obtained by adding the contributions from each part of the ion beam.

The sampling of Θ and Φ was done using equal increments of angle. This does not result in spherical symmetry for the probability of the distribution of the vector AG unless a weighting proportional to $\cos \Phi$ is assigned to each m^*.

Fig. 4 shows the shape of the peaks computed from the data:

$$T = 0.1 \text{ eV}, \quad E_0 = 8000 \text{ eV}, \quad m_1 = 79, \quad m_2 = 52.$$

Fig. 4 A assumes all the daughter ions are collected and Fig. 4 B includes the effect of discrimination by a collector slit of length 0.080″, the actual collector slit length of the M.S. 9 mass spectrometer used in this work. The intensity of both these peaks

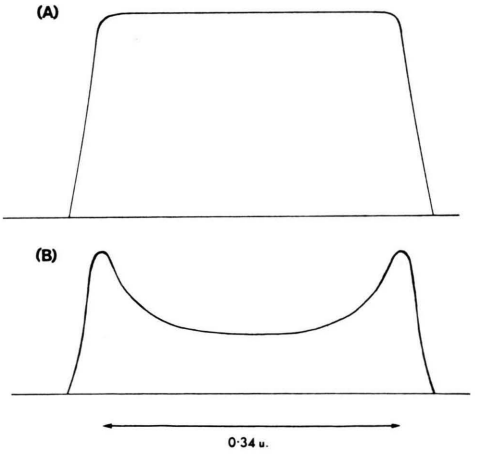

Fig. 4. Computed peak shapes for a release of 0.1 eV kinetic energy (A) Assuming collection of all fragment ions. (B) Assuming discrimination by a collector slit of length 0.080″.

falls from maximum to zero in approximately 0.03 u. The slope on the sides of "flat-topped meta-stable peaks" found in mass spectra is usually five to ten times less.

If the data $T = 0.001$ eV, $E_0 = 8000$ eV, $m_1 = 79$, $m_2 = 52$ are used a narrow "flat-topped" peak is still obtained, the width of the flat-top being 0.03 u and the sides falling from maximum to zero in 0.006 u.

For ion beams produced by electron bombardment, assuming the ionization chamber temperature to be 500 °K corresponds to a thermal ion energy of 0.043 eV. There is also an energy spread of about the same amount due to formation of ions in different parts of the ionization chamber. In a double-focussing mass spectrometer such as the M.S. 9 the effects of such energy spread are reduced by a factor of 100 – 200. Thus, for a decomposition involving no release of kinetic energy, the effective value of T is about $10^{-3} - 5 \times 10^{-4}$ eV.

In the foregoing treatment of the meta-stable decomposition process the ion beam from the source slit of the mass spectrometer has been assumed to be infinitely narrow in the y-direction. The effect on the "meta-stable peak" of introducing a divergence angle can also be included in the computation. In Fig. 5 a meta-stable ion m_1^+ of energy E_0 diverging from the slit S at an angle ε undergoes decomposition at A, at a distance d from the magnet. If the resulting path of m_2^+ is at an angle α (measured in the xy plane) to the original direction of m_1^+ then the radius of curvature R_2 of m_2^+ on entering the magnet can be calculated from Eqs. (1) and (2) as before, if "d" is replaced by d_x and "α" is replaced by $(\alpha + \varepsilon)$.

From the geometry of Fig. 5 it can be shown that

$$d_x = d + (d_0 - d)\ \mathrm{tg}\ \varepsilon\ \cot(\varepsilon + \alpha).$$

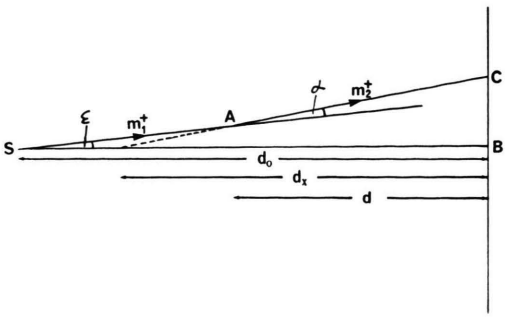

Fig. 5. The effect of divergence of the ion beam on the path of the fragment ion.

Thus it is possible to perform calculations to ascertain the effect on the peak of introducing typical values of ε ($< 10^{-2}$ radians). These calculations show that the peak amplitudes and shapes shown in Fig. 4 are still produced, together with very weak tails on each side of the peak. The intensity of the tails is only 2 – 3 per cent of the maximum peak intensity dying away to zero over a mass range which increases with the value of ε.

d) Decomposition within the dispersing magnetic field

COGGESHALL [21] and NEWTON [22] have considered the dissociation of ions within the magnet of a DEMPSTER type 180° single focussing mass spectrometer. Both these workers considered decompositions of specific ion species and included in their calculations estimates of the half-lives involved. The present work has considered decompositions occurring in a sector magnet as shown in Fig. 6. In this figure, the meta-stable ion m_1^+, energy E_0, is shown entering the magnet normally and decomposing at A, with no release of internal energy, after following a path BA,

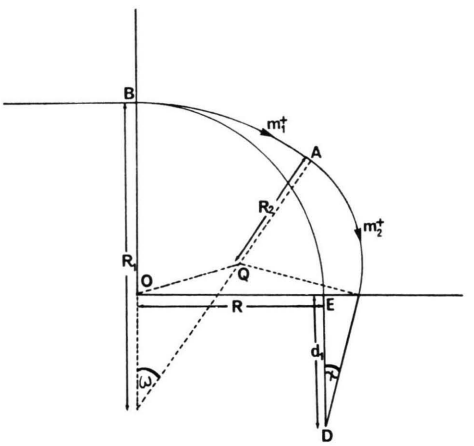

Fig. 6. Schematic diagram showing decompositions occurring in the magnetic field with no release of kinetic energy.

radius R_1. The resultant daughter ion m_2^+ has a path of radius R_2, leaves the magnet and enters the collector slit at D. It is supposed that simultaneously an ion m^{*+}, energy E_0, enters and leaves the magnet normally having followed the radius R. The relationship between m^* (the apparent mass of the meta-stable ion), E_2 (the energy of m_2), E_0, R_2 and R

[21] N. D. COGGESHALL, J. Chem. Phys. **37**, 2167 [1962].

[22] A. S. NEWTON, J. Chem. Phys. **44**, 4015 [1966].

can be deduced as before

$$m^* = m_2 \frac{E_2}{E_0} \frac{R^2}{R_2^2}. \quad (15)$$

R_1 and R_2 are related by:

$$R_1 = R_2 \frac{m_1}{m_2} \sqrt{E_0/E_2} \quad (16)$$

and for a given value of ω the following geometrical relationships can be deduced from Fig. 6:

$$R = (R_1 - R_2) \sin\omega + R_2 \cos\psi - d_1 \operatorname{tg}\psi, \quad (17)$$

$$R_1 - R = (R_1 - R_2) \cos\omega - R_2 \sin\psi. \quad (18)$$

These enable R_2 to be evaluated.

Thus by taking in succession the whole range of values for ω and assuming equal probabilities for decompositions at any time during the transit of m_1^* through the magnet the values of m^* can be calculated and an intensity distribution obtained. Two such distributions resulting from the hypothetical decompositions:

$$100^+ \rightarrow 50^+ + 50$$

and

$$100^+ \rightarrow 99^+ + 1$$

occurring in the magnet without release of energy were considered. The result shows the distribution to take the form of a continuum from m_2^2/m_1 to m_1, the intensity rising slightly at each limit. Fig. 6 shows the flight paths of ions m_1^+ and m_2^+ when there is no release of kinetic energy. We have also considered the general case of a spreading ion beam and a release of kinetic energy. The result is very similar though the continuum now extends slightly beyond each of the above limits. The calculations were done using distances estimated from the geometry of the M.S. 9 mass spectrometer which has a magnet analyser tube of outer radius 12.75″.

In terms of Fig. 6, a daughter ion from the decomposition will hit the wall of the tube if $(OQ + R_2)$ is greater than the outer radius of the magnet tube. This condition is due to COGGESHALL [21]. In geometrical terms cut off occurs when:

$$R_2 + ((R_1 - R_2)^2 + (R_1 - R)^2 - 2(R_1 - R_2)(R_1 - R)\cos\omega)^{1/2} > 12.75''.$$

The calculations showed that for a large mass change on decomposition, only values of ω near 0° and near 90° satisfy the condition for transmission and collection.

For a mass change of $\sim 1\%$ however all values of ω satisfy the condition.

e) Decompositions in the field free region before the collector

In part c) of this paper it was shown that meta-stable ions m_1^+ decomposing with the release of internal energy give rise to daughter ions m_2^+ the motion of which can be described by considering the velocity V_z in the z direction and the velocity V_α along a line making an angle α with the x direction and lying in the xy plane. A daughter ion formed in the field free region in front of the collector slit by such a decomposition will in general have a component of velocity in the xy plane making an angle α with the original direction of the meta-stable ion m_1^+. m_2^+ will therefore be collected at a different value of magnetic field from m_1^+. The apparent mass of m_2^+ is given by:

$$m^* = \frac{m_1 R^2}{R_1^2}.$$

The conditions for collection of this ion are shown in Fig. 7 where R_1 is the radius of the path of m_1^+ in the magnet when m_2^+ is collected. R_1 can be calculated from the geometrical relationships:

$$R_1 \cos(\alpha - \delta) = R + (d_1 - d) \operatorname{tg}(\alpha - \delta) - d \operatorname{tg}\gamma, \quad (19)$$

$$R_1 \sin(\alpha - \gamma) = R - R_1. \quad (20)$$

d is the distance from the collector at which the decomposition occurs.

No computation has been attempted from these equations in this work, though it may be said that the intensity distribution must take the form of a tail on each side of the m_1 peak observed in the mass spectrum. The spread of the tails will increase with increasing kinetic energy of separation and provides a means of estimating the magnitude of this released energy.

Experimental

Several experiments were carried out in attempts to verify the theoretical predictions. The experiments are described below. The letter at the commencement of each section refers to the corresponding section in the theoretical part of the paper.

a) Discussion is included with d) below.

b) The peak shapes observed due to decomposition in the electrostatic analyser have already been described [10].

c) Discriminations due to the finite collector slit length have been investigated by comparing the

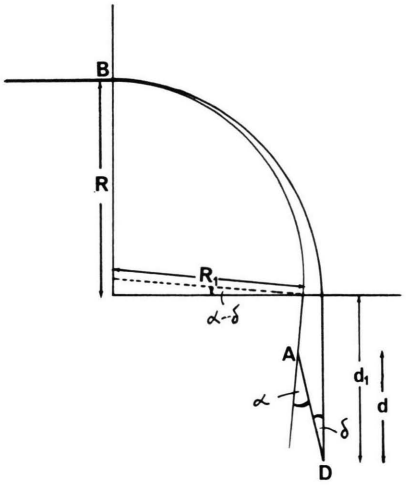

Fig. 7. Schematic diagram showing decompositions occurring in the field free region in front of the collector including the effects of kinetic energy release.

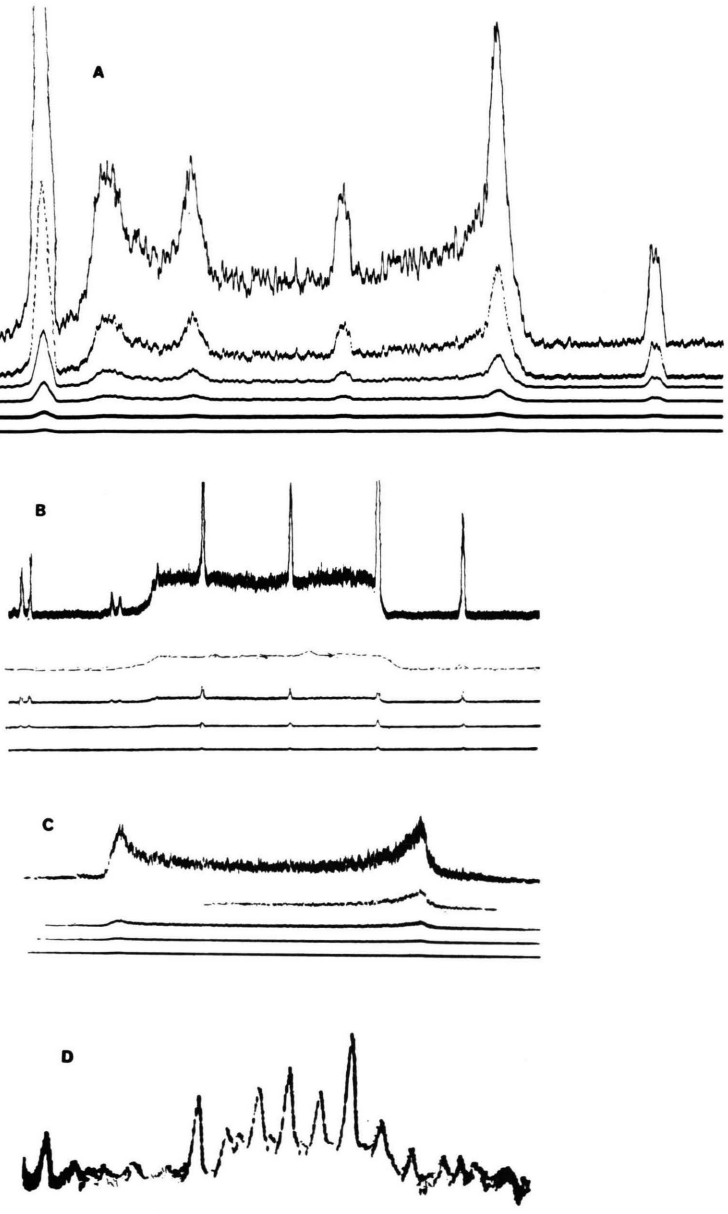

Fig. 8. Peak shapes obtained for the "meta-stable peak" from $C_6H_6^{++} \rightarrow C_5H_3^+ + CH_3^+$ in mass spectrometers with different lengths of collector slit.

shape of the "broad meta-stable peak" which occurs in the mass spectrum of benzene and due to the decomposition:

$$C_6H_6^{++} \rightarrow C_5H_3^+ + CH_3^+ + \sim 2.8 \text{ eV}$$

in three different mass spectrometers. These were the M.S. 9 having a collector slit length of 0.080″, the M.S. 12 [23] of slit length 0.200″ and a single-focussing mass spectrometer, built to the design of GRAHAM, HARKNESS and THODE [24] (of 6″ radius in the magnetic field) of slit length 0.300″. Fig. 8 A shows the peak shape in the M.S. 9 at 8 kV accel-

[23] A. E. BANNER, R. M. ELLIOTT, and W. KELLY, Gas Chromatography 1964, Proc. of 5th Symposium Brighton 1964, Butterworths London 1965, p. 180.

[24] R. L. GRAHAM, A. L. HARKNESS, and H. G. THODE, J. Sci. Instrum. **24**, 119 [1947].

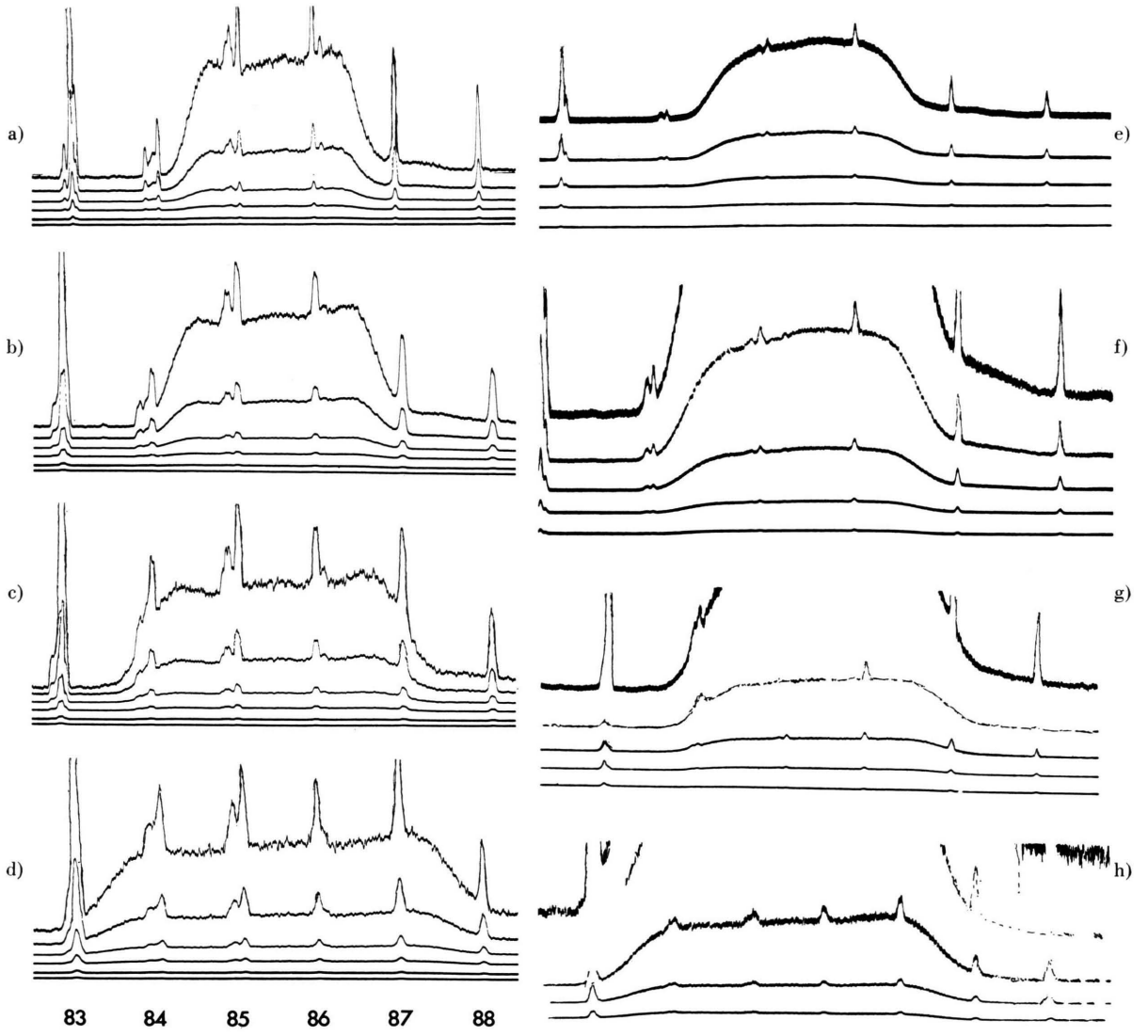

Fig. 9. Peak shapes obtained for the "meta-stable peak" from $C_6H_5NO_3^{+\cdot} \rightarrow C_6H_5O_2^{+} + NO\cdot$ in mass spectrometers with different lengths of collector slit and at different accelerating voltages.

erating voltage and Fig. 8 B the peak shape in the M.S. 12 also at 8 kV. Fig. 8 C shows the M.S. 12 plot at an accelerating voltage of 2 kV and Fig. 8 D the plot in the 6″ radius instrument also at 2 kV. The lower discrimination against ions falling near the mass m_2^2/m_1 in the instruments having the longer collector slits is clearly visible. The M.S. 9 and M.S. 12 instruments are particularly suitable for comparison since their magnet sector geometries are identical. Further evidence of the effect of slit length is shown in Fig. 9 which gives the shape of the "meta-stable peak" in the spectrum of o-nitro phenol due to the decomposition:

$$C_6H_5NO_3^{+\cdot} \rightarrow C_6H_5O_2^{+} + NO^{\cdot} + \sim 0.75 \text{ eV}.$$

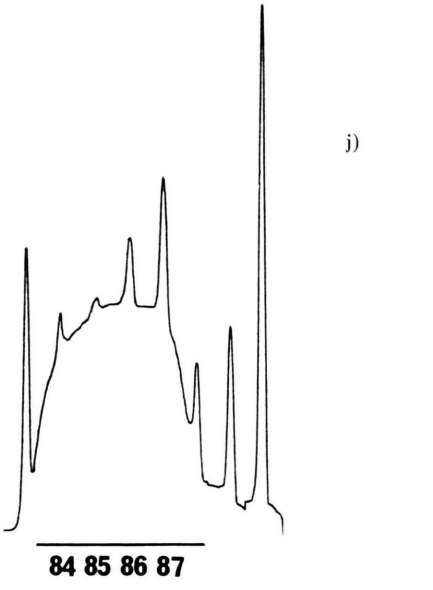

Figs. 9 a, b, c and d show the peak shape obtained in the M.S. 9 at voltages 8, 6, 4 and 2 kV and Figs. 9 e, f, g, and h the corresponding peak shapes at the same accelerating voltages in the M.S. 12. Fig. 9 j shows the peak shape obtained on the 6″ radius single-focussing sector instrument at an accelerating voltage of 2 kV. These plots show that the wide "flat topped" peak obtained at 2 kV in the M.S. 9 becomes progressively more rounded either as the accelerating voltage is changed or as the slit length is increased by changing to another instrument.

A characteristic of all the broad "meta-stable peaks" obtained in practice is that the slope of the sides is lower than in a normal ion peak. The computer calculations given in c) of the theoretical part of this paper predict peaks with steeply sloping sides, even when there is no discrimination, and an infinitely long slit is employed. A typical "narrow meta-stable peak" which can be used to compare with the shape predicted by theory is for example that at m/e 34.2 in the spectrum of pyridine and due to the transition:

$$79^+ \rightarrow 52^+ + 27\,.$$

It has a width at half height measured on the M.S. 9 of 0.17 u some six times greater than the computed peak width. This must mean that there is a small range of kinetic energy released in the fragmentation and this will have the effects of reducing the slope on the sides of the peak and of rounding the flat top predicted by theory. A similar spread of kinetic energies about the mean value might be expected in those cases where kinetic energy release is observed. This may explain why more examples of "dished-topped meta-stable peaks" rather than "flat-topped" are not observed, and why the observed slopes of the sides of the peaks are always lower than those computed on the assumption that all decompositions

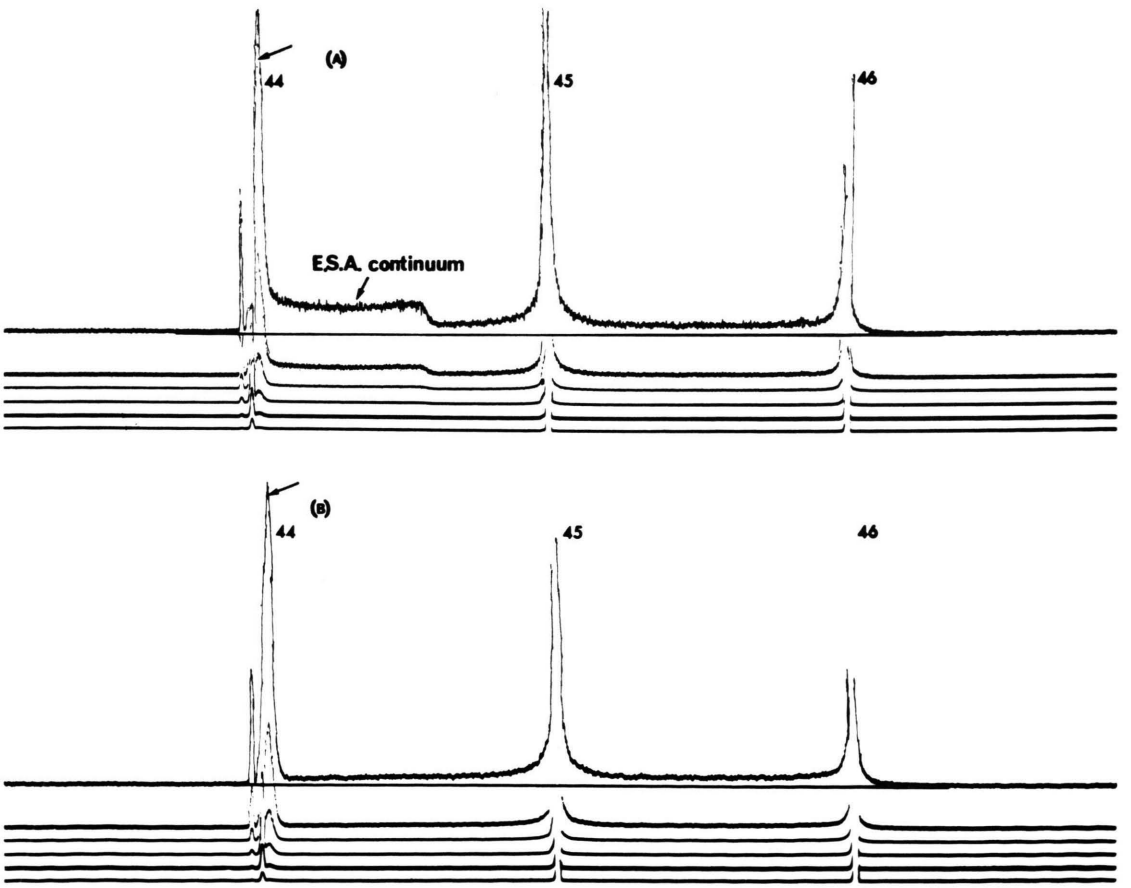

Fig. 10. Part of the mass spectrum of ethanol showing the continuum due to decomposition of meta-stable ions in the magnetic field and the distortion due to decompositions in the accelerating region.

release exactly the same amount of energy. The computer plots were, of course, obtained on the assumption of a long half-life for the meta-stable ion. Introduction of a shorter half-life into the equations has no effect on the shape of the sides of the peaks when decompositions occurring before the magnetic analyser are considered, and it was shown originally by COGGESHALL [21] that decompositions within the magnetic analyser tend only to produce asymmetry in the observed "meta-stable peak". Variation of divergence angle of the beam, release of energy in 3-dimensions and slit discriminations also do not produce the required slope on the sides of the peaks. The fringe magnetic field also would not be expected to produce the desired slope; it is shown later that for decompositions occurring during passage through the main magnetic field the effect produced is to form the continuum between m_2^2/m_1 and m_1 and the effect of the fringe field would be expected to be qualitatively similar. It is, however, easily possible to produce any required slope on the sides of the "flat topped" peak by assuming an appropriate energy distribution.

d) Fig. 10 shows part of the mass spectrum of ethanol obtained on the M.S. 9 mass spectrometer. The "meta-stable peak" due to the transition:

$$C_2H_6O^{+\cdot} \rightarrow C_2H_5O^+ + H\cdot$$

is clearly visible at mass 44 and is indicated by an arrow. The continuum which manifests itself as a displacement of the zero line between masses 44 and 46 is clearly visible. Fig. 10 A was obtained with the ion beam passing near one edge of the energy selector slit between the electrostatic and magnetic analysers. As a result some of the daughter ions produced by decompositions near the exit end of the electrostatic analyser can be seen producing the plateau-like "meta-stable peak" which has previously been discussed [10]. Fig. 10 B shows the spectrum obtained when the deflecting voltage is adjusted so that the ion beam passes close to the other edge of the energy selector slit so that no ions which have lost energy before this point are transmitted through the instrument. The continuum due to decompositions in the magnet remains clearly visible. A decomposition involving only a small mass change was used as illustration since only under these conditions is the continuum likely to be intense enough for detection. Also, as there is no "cut-off" by the magnet tube for small mass changes all the products of decompositions occurring in the magnet sector are transmitted and there is no break in the continuum midway between m_2^2/m_1 and m_1.

Comparing the lower mass side of the peaks at masses 46 and 45, it can be seen that there is a small distortion near the baseline on the low mass side of mass 45. This is most clearly observed on the lower sensitivity traces. This distortion is thought to be due to ions which have decomposed in the accelerating field near to the ionisation chamber as discussed theoretically in Section a). Theory suggests that a corresponding distortion would be expected on the high mass side of m^* (the peak marked with an arrow). However, ions appearing at this position on the mass scale would have lost sufficient energy to prevent their passage through the electrostatic analyser.

e) In order to demonstrate the predicted broadening of a mass peak due to decomposition between

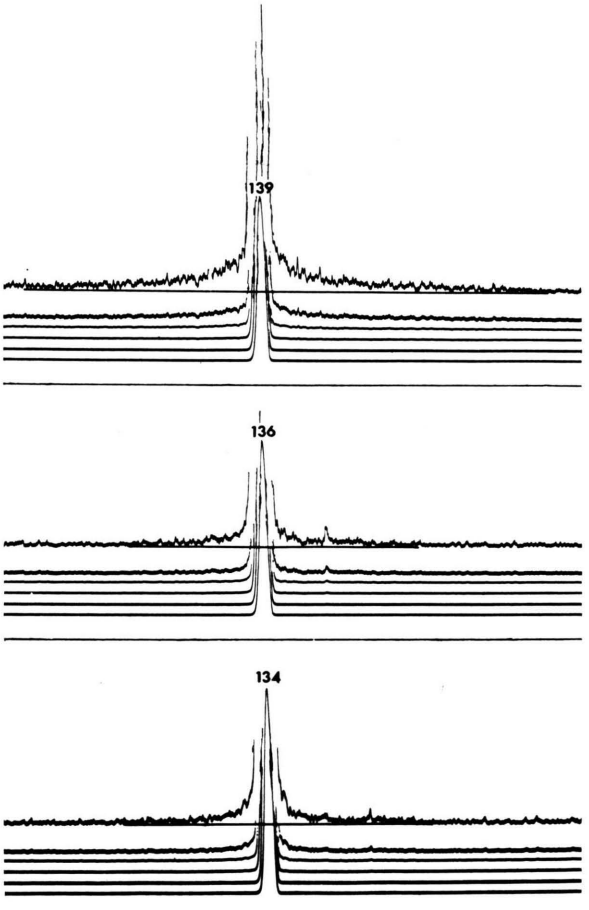

Fig. 11. Effect of decompositions with release of kinetic energy in the field-free region in front of the collector.

the magnetic analyser and collector slit, the molecular peak of o-nitro phenol (mass to charge ratio 139) was compared in width with the xenon peaks $^{136}Xe^{+\cdot}$ and $^{134}Xe^{+\cdot}$. The molecular ion of o-nitro phenol, as has been mentioned above, decomposes with loss of mass 30 and simultaneous release of ~ 0.75 eV of kinetic energy. Two xenon peaks were used for comparison to ensure that there was no mass discrimination effect itself giving rise to peak broadening. The peaks obtained are shown in Fig. 11. The widths of the three peaks were measured at several percentages of their heights and in all cases the peak at mass 139 was broader than the other two. For example, the widths of the three peaks of masses 139, 136 and 134 at $\frac{1}{300}$ of peak height are respectively 0.0322 u, 0.0294 u and 0.0290 u. This means that the resolving power of a mass spectrometer is reduced whenever an ion decomposing with release of kinetic energy is being observed. Using the above figures, it is seen that on a definition of resolving power taken on the 0.6% valley definition, the maximum obtainable resolving power in an M.S. 9 for the 139 peak in o-nitro phenol would be about 50,000. The skirts on the peak extend much further than do the corresponding skirts on the xenon peaks. Thus an organic molecule decomposing with loss of kinetic energy would also be quite unsuitable for experiments in a mass spectrometer of high abundance sensitivity.

It has proved possible to distinguish the effects of decompositions in the various regions making up the ion path in a mass spectrometer. It has not been possible to exactly match observed "meta-stable peak" shapes in all cases without invoking the release of a range of kinetic energies in some transitions.

The authors wish to acknowledge the help received from Mr. E. G. H. Crouch in programming the computer and Mr. R. Coombs for running 2 sets of spectra on the MS 12 mass spectrometer.